


RESEARCH

Open Access



# Analyzing radiowave multiple diffraction from a low transmitter in vegetated urban areas using a spherical-wave UTD–PO approach

José Lorente-López<sup>1\*</sup> , José-Víctor Rodríguez<sup>1†</sup>, María-Teresa Martínez-Inglés<sup>2†</sup>,  
Jose-Maria Molina Garcia-Pardo<sup>1†</sup>, Ignacio Rodríguez-Rodríguez<sup>3</sup> and Leandro Juan-Llácer<sup>1</sup>

<sup>†</sup>José-Víctor Rodríguez, María-Teresa Martínez-Inglés and Jose-Maria Molina Garcia-Pardo contributed equally to this work.

\*Correspondence:  
jose.lorente2@edu.upct.es

<sup>1</sup> Departamento de Tecnologías de la Información y las Comunicaciones, Universidad Politécnica de Cartagena, Antiguo Cuartel de Antigones, 30202 Cartagena, Murcia, Spain

<sup>2</sup> Departamento de Ingeniería y Técnicas Aplicadas, University Center of Defense Ministerio de Defensa-Universidad Politécnica de Cartagena, San Javier Air Force Base, 30720 Santiago de la Ribera, Murcia, Spain

<sup>3</sup> Departamento de Ingeniería de Comunicaciones, Universidad de Málaga, Avda. Cervantes, 2, 29071 Málaga, Málaga, Spain

## Abstract

This article introduces a uniform theory of diffraction–physical optics (UTD–PO) formulation for analyzing radiowave multiple diffraction emanating from trees and buildings in green urban areas, considering illumination from a low transmitter and assuming spherical-wave incidence. Based on Babinet’s principle, this solution models buildings as rectangular sections and accounts for the influence of tree crowns (assuming these rise above the average rooftop height) by incorporating appropriate attenuation factors/phasors into the diffraction phenomena of buildings. The validation of the formulation is achieved through measurements made at the 39 GHz 6G mmWave frequency on a scale model of a green urban environment comprising bonsai trees and bricks. The main advantage of the proposed solution is that the calculations only include single diffractions due to recursion, circumventing the need to use higher-order diffraction terms in the diffraction coefficients, thus reducing the computation time and power. Our results may be beneficial for the design of mobile communication systems, including 6G networks, situated in green urban areas and with transmission source positioned lower than the surrounding infrastructure.

**Keywords:** Negative incidence, Mobile communication, Multiple diffraction (MD), Uniform theory of diffraction (UTD), vegetation

## 1 Introduction

The analysis of radiowave propagation in urban environments is crucial for the efficient design and deployment of current and future wireless communication systems, including emerging technologies like 6G networks. This importance stems from several intrinsic characteristics of urban environments and the nature of radiowaves. Urban environments present unique challenges for radiowave propagation due to their densely populated and structurally complex nature. Buildings, vehicles, vegetation, and other urban structures can cause attenuation, diffraction, reflection, and scattering of radiowaves [1]. Therefore, this can lead to significant issues such as signal attenuation and multipath fading, adversely affecting the quality and reliability of wireless communications [2]. Moreover, with the advent of advanced technologies like 6G networks, which

promise ultra-high data speeds and low latency, a precise understanding of wave propagation in urban settings becomes even more critical. 6G networks are likely to operate at higher frequencies, such as millimeter and terahertz bands, which are more susceptible to propagation losses and atmospheric absorption [3]. Furthermore, a detailed analysis of radiowave propagation in urban environments is crucial for the modeling and simulation of wireless networks, allowing researchers and engineers to predict network performance and identify potential issues before actual deployment [4]. Meanwhile, whether in urban or semi-urban settings, such a study must also take multiple diffraction into consideration as radiowaves interact with the rooftops in a residential environment. This is a primary cause of signal attenuation in such areas, in addition to free-space loss and the attenuation caused by ground-level diffraction [5]. To further elucidate this phenomenon, various works have performed analyses of multiple wave diffraction in urban settings through the lenses of a variety of frameworks, from physical optics [6, 7] to the uniform theory of diffraction (UTD) [8, 9]. On the other hand, for an optimal design of advanced wireless communications networks in urban environments, it may be beneficial to integrate recent advancements in antenna design and propagation modeling. In this sense, for example, the incorporation of fractal antennas, known for their ability to operate at multiple frequencies due to their self-similar design, offers an enhanced bandwidth and multi-band functionality that is crucial for the complex urban environments where 6G networks will operate. Such antennas are particularly advantageous in densely built-up areas as they allow for more flexible frequency usage and can enhance signal penetration and distribution through challenging urban topographies [10–13]. Furthermore, in the same vein, it is also worth mentioning the fractal-wavelet modeling approach, which, applying fractal geometry combined with wavelet transforms, provides a powerful method for analyzing and simulating the propagation characteristics in urban environments. This technique takes advantage of the fractal nature of urban landscapes, where the distribution of buildings and vegetation often exhibits self-similarity at various scales. This way, by employing wavelet transforms, this method can efficiently decompose the radiowave interactions into different scales and frequencies, allowing for a more precise and detailed analysis of wave propagation and multi-path effects [14–19].

Moreover, numerous studies [20–24] have examined in detail how radiowave diffraction is specifically affected by trees, which create natural obstacles. Crucially, the study of radiowave diffraction in residential areas that comprise both vegetation and buildings must consider the attenuation effects due to trees, especially their canopies. Prior work in this field has generally concentrated on millimeter-wave [25] and UHF frequencies [26–28], thereby assuming plane-wave incidence over obstacle arrays. Yet, in the context of micro- or picocellular systems, the transmission antennas are often situated in or around vegetated urban areas; thus, basing on spherical-wave incidence may offer more realistic and accurate estimations of multi diffraction attenuation. On the other hand, the works presented in [25–28] consider that the transmitting antenna is located above the average height of the buildings and trees comprising the environment under study, so that the incidence of the waves on the diffracting elements is assumed to have a positive angle. Nevertheless, in the micro- and picocellular environments mentioned above, the transmitting source may be positioned below the average height of buildings and trees. In addition, this scenario may also arise when considering the uplink established

from a user at street level to the nearest receiving antenna located on top of a surrounding building bounded by trees. Therefore, in these cases, the incidence on the obstacles would occur with a negative angle and, therefore, the consequent analysis of the multiple diffraction caused by the diffracting elements requires a specific formulation developed for this purpose. Finally, it is worth mentioning that the formulations proposed in [25, 26, 28] consider buildings modeled as knife edges, being that the assumption of more complex modeling as rectangular sections (plateaus) can yield more realistic attenuation results when compared to experimental measurements [29]. In this sense, the work presented in [27] does model buildings as blocks, but, on the one hand, as already mentioned, it assumes only a positive plane-wave incidence on the obstacles and, on the other hand, the proposed formulation presents as its main limitation the need to incorporate higher-order terms in the diffraction coefficients, which results in a higher computational cost.

In line with this, we here introduce a spherical-wave UTD–PO formulation for the estimation of radiowave multiple diffraction attenuation in urban areas comprising both houses and trees and with the transmitting antenna located below the average height of the obstacles (i.e., negative incidence). Moreover, this formulation models the buildings as rectangular structures, making the results more realistic. As our approach is recursive, it offers the key advantage of a simplified calculation process as merely single diffraction calculations are required, eliminating the need to integrate higher-order terms into the diffraction coefficients, significantly lessening the computational burden. Furthermore, we use 39 GHz 6G mmWave frequency measurements conducted on a scaled model consisting of bricks and bonsai trees to empirically validate our theoretical estimations. It is noteworthy that we obtain our empirical results from a controlled laboratory experiment; according to [30], this permits precise parameter control while also delivering insights that can be applied to radiowave propagation situations in the real world.

## 2 Propagation environment

Figure 1 (top) presents the propagation scenario investigated in this study, comprising a group of  $n$  equally high buildings beside trees.

We assume a constant space  $z$  between each building/tree pair and a tree canopy height exceeding the average building height. Consequently, the direct ray (LOS path)

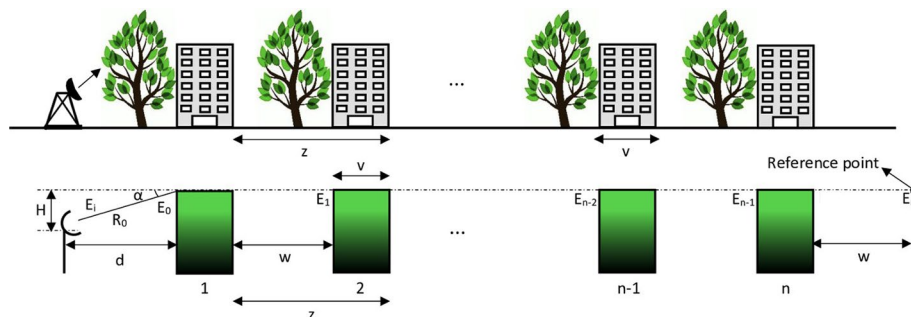


**Fig. 1** Considered propagation scenario of a vegetated urban area, with buildings and trees in rows (top); the same environment, with the buildings (including the presence of trees) represented rectangular shapes (bottom)

for the spherical wave impinging across the first obstacle with a negative incident angle  $\alpha$  is obstructed by the canopies. In addition, the transmitting antenna, with a height  $H$  (negative) below the average building height, is sited a set distance  $d$  from the obstacle array; thus, it is impinged by a spherical wave. The bottom of Fig. 1 illustrates a setting wherein every building/tree pair is represented by a black and green block (rectangular section) with the width  $v$ ; this block combines the effect of the buildings and trees in terms of the diffraction phenomena. Hereby, we assume a constant spacing of  $w$  between the black and green rectangles, i.e.,  $v + w = z$ .

### 3 Theoretical formulation

We ground in the spherical-wave UTD-PO solution for multiple diffraction by a rectangular section illuminated from below by a transmitter [31] and also draw on [32]’s approach to consider the attenuation influence of rectangular buildings and trees (although the prior work involved positive incidence). Based on that, we introduce a new UTD-PO theoretical formulation for multiple diffraction analysis accounting for tree canopies beside rectangular buildings and a negative incidence.

Beginning with the initial case of  $n = 1$ , Fig. 2 shows the decomposition, via Babinet’s principle, of the analysis of this scenario into additions and subtractions of different geometries incorporating solely diffraction over knife edges. In particular, the first geometry is a double diffraction with negative incidence (whereby the adjacent tree canopy is considered by including the corresponding attenuation factor and phasor); the subtraction of the two remaining geometries (respectively, representing positive incidence over one and two knife edges) presents the reflection generated by the top of the rectangular section modeling the building.

Hence, we can determine the total field arriving at the reference point in Fig. 2 ( $E_1$ , also termed  $E_{10}$  in line with the formulation for  $n > 1$ , as explained in the following) using the formula:

$$E_1 = E_{10} = E'_{10} \pm E''_{10} - E'''_{10} \tag{1}$$

where “+” is for hard polarization and “-” is for soft polarization, and

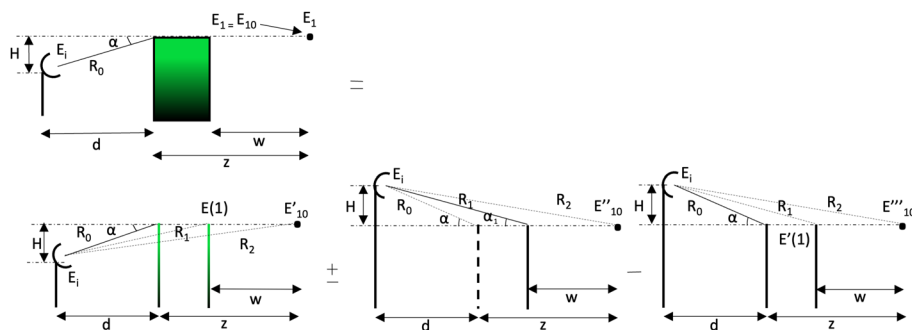


**Fig. 2** Considered propagation scenario for vegetated urban areas for  $n = 1$ , demonstrating the breakdown, via Babinet’s principle, of this scenario into knife-edge geometries

$$E'_{10} = \frac{1}{2} \left[ \frac{E_i}{R_0} A e^{-jkR_0} \sqrt{\frac{R_0}{(v+w)(R_0+v+w)}} D\left(\phi = \frac{3\pi}{2}, \phi' = \frac{\pi}{2} + \alpha, L = \frac{R_0(v+w)}{R_0+(v+w)}\right) \right. \\ \left. e^{-jk(v+w)} e^{-j\Delta k \Delta d} + E(1) \sqrt{\frac{R_0}{w(R_0+w)}} D\left(\phi = \frac{3\pi}{2}, \phi' = \frac{\pi}{2} + \alpha, L = \frac{R_0 w}{R_0+w}\right) e^{-jkw} \right] \quad (2)$$

where  $E_i$  is the spherical source's relative amplitude (here assumed to be 1),  $k$  is the wavenumber,  $D(\phi, \phi', L)$  is the UTD diffraction coefficient for a knife edge, as per [33], and

$$R_0 = \sqrt{H^2 + d^2} \quad (3)$$

$$\alpha = \arctan\left(\frac{H}{d}\right) \quad (4)$$

$$E(1) = \frac{E_i}{R_0} A e^{-jkR_0} \sqrt{\frac{R_0}{v(R_0+v)}} D\left(\phi = \frac{3\pi}{2}, \phi' = \frac{\pi}{2} + \alpha, L = \frac{R_0 v}{R_0+v}\right) e^{-jkv} e^{-j\Delta k \Delta d} \quad (5)$$

$$E''_{10} = \frac{E_i}{R_2} e^{-jkR_2} + \frac{E_i}{R_1} e^{-jkR_1} \sqrt{\frac{R_1}{w(R_1+w)}} D\left(\phi = \frac{3\pi}{2}, \phi' = \frac{\pi}{2} + \alpha_1, L = \frac{R_1 w}{R_1+w}\right) e^{-jkw} \quad (6)$$

$$R_1 = \sqrt{H^2 + (d+v)^2} \quad (7)$$

$$R_2 = \sqrt{H^2 + (d+v+w)^2} \quad (8)$$

$$\alpha_1 = \arctan\left(\frac{H}{(d+v)}\right) \quad (9)$$

$$E'''_{10} = \frac{1}{2} \left[ \frac{E_i}{R_0} e^{-jkR_0} \left( \frac{R_0}{R_2} e^{-jk(R_2-R_0)} \right. \right. \\ \left. \left. + \sqrt{\frac{R_0}{(v+w)(R_0+v+w)}} D\left(\phi = \frac{3\pi}{2}, \phi' = \frac{\pi}{2} + \alpha, L = \frac{R_0(v+w)}{R_0+(v+w)}\right) e^{-jk(v+w)} \right) \right. \\ \left. + E'(1) \left( \frac{R_0}{R_1} e^{-jk(R_2-R_1)} + \sqrt{\frac{R_0}{w(R_0+w)}} \right) \right. \\ \left. \times D\left(\phi = \frac{3\pi}{2}, \phi' = \frac{\pi}{2} + \alpha, L = \frac{R_0 w}{R_0+w}\right) e^{-jkw} \right] \quad (10)$$

$$E'(1) = \frac{E_i}{R_0} e^{-jkR_0} \left[ \frac{R_0}{R_1} e^{-jk(R_1-R_0)} + \sqrt{\frac{R_0}{v(R_0+v)}} D\left(\phi = \frac{3\pi}{2}, \phi' = \frac{\pi}{2} + \alpha, L = \frac{R_0 v}{R_0+v}\right) e^{-jkv} \right] \quad (11)$$

$$R'_1 = \sqrt{H^2 + (d+w)^2} \quad (12)$$

Further,  $\Delta d$  is the average propagation path length through the tree canopy,

$$A = \exp\left(-\frac{L_v}{8.686}\right) \tag{13}$$

and  $L_v$  is the attenuation (in dB) due to vegetation (relative to free space), thus

$$L_v = \begin{cases} 26.6f^{-0.02}\Delta d^{0.5} & \text{trees out-of-leaf} \\ 15.6f^{-0.009}\Delta d^{0.5} & \text{trees in-leaf} \end{cases} \tag{14}$$

assuming the COST235 model [34], being that  $f$  is in MHz and  $\Delta d$  is in m,

$$\Delta k = k(n_R - 1) \tag{15}$$

where  $n_R$  is the real part of the refractive index of the leaves [35]

$$n_R = \sqrt{\varepsilon' + n_I^2} \tag{16}$$

and  $n_I$  is the imaginary part of the refractive index of the leaves

$$n_I = \frac{L_v}{8.686} \quad \text{when} \quad \Delta d = 1m \tag{17}$$

where  $\varepsilon'$  is the real part of the leaves' relative permittivity

$$\varepsilon' = A' - B'm_d \tag{18}$$

where

$$0.1 \leq m_d \leq 0.5 \tag{19}$$

The coefficient values for  $A'$  and  $B'$  are presented in [35]. Here, we use typical values of  $m_d = 0.3$ ,  $A' = 8.8$  and  $B' = 4.3$ .

Thus, for  $n \geq 1$ , based on the previous analysis and the recursive UTD-PO approach based on virtual spherical sources introduced in [9], we may obtain the total field  $E_n$  arriving at the reference point in Fig. 1 as

$$E_n = \frac{1}{n} \sum_{m=0}^{n-1} E_{nm} \tag{20}$$

$$E_{nm} = E'_{nm} \pm (E''_{nm} - E'''_{nm}) \tag{21}$$

$$E'_{nm} = \frac{1}{2} \left[ \frac{E_i}{R_0} A e^{-jkR_0} \sqrt{\frac{R_0}{(v+w')(R_0+v+w')}} D\left(\phi = \frac{3\pi}{2}, \phi' = \frac{\pi}{2} + \alpha, L = \frac{R_0(v+w')}{R_0+(v+w')}\right) \right. \\ \left. \times e^{-jk(v+w')} e^{-j\Delta k \Delta d} + E(1) \sqrt{\frac{R_0}{w'(R_0+w')}} D\left(\phi = \frac{3\pi}{2}, \phi' = \frac{\pi}{2} + \alpha, L = \frac{R_0 w'}{R_0+w'}\right) e^{-jk w'} \right] \tag{22}$$

where  $R_0$ ,  $\alpha$  and  $E(1)$  are to be considered as in (3), (4), and (5), respectively,  $\Delta d$  is once more the average propagation path length through the tree canopy,  $A$  is to be considered as in (13), and

$$E_i = \begin{cases} 1 & \text{if } m = 0 \\ E_m R_0 e^{jkR_0} & \text{if } m \neq 0 \end{cases} \tag{23}$$

$$w' = (n - m)w + (n - m - 1)v \tag{24}$$

$$E''_{nm} = \frac{E_i}{R_2} e^{-jkR_2} + \frac{E_i}{R_1} e^{-jkR_1} \sqrt{\frac{R_1}{w'(R_1+w')}} \times D\left(\phi = \frac{3\pi}{2}, \phi' = \frac{\pi}{2} + \alpha_1, L = \frac{R_1 w'}{R_1+w'}\right) e^{-jkw'} \tag{25}$$

with  $E_i$  as in (23), and  $R_1$  and  $\alpha_1$  as in (7) and (9), respectively, and

$$R_2 = \sqrt{H^2 + (d + v + w')^2} \tag{26}$$

and, finally,

$$E'''_{nm} = \frac{1}{2} \left[ \frac{E_i}{R_0} e^{-jkR_0} \left( \frac{R_0}{R_2} e^{-jk(R_2-R_0)} + \sqrt{\frac{R_0}{(v+w')(R_0+v+w')}} D\left(\phi = \frac{3\pi}{2}, \phi' = \frac{\pi}{2} + \alpha, L = \frac{R_0(v+w')}{R_0+(v+w')}\right) e^{-jk(v+w')} \right) + E'(1) \left( \frac{R_0}{R'_1} e^{-jk(R_2-R_1)} + \sqrt{\frac{R_0}{w'(R_0+w')}} D\left(\phi = \frac{3\pi}{2}, \phi' = \frac{\pi}{2} + \alpha, L = \frac{R_0 w'}{R_0+w'}\right) e^{-jkw'} \right) \right] \tag{27}$$

with  $E'(1)$  as in (11),  $E_i$  as in (23), and

$$R'_1 = \sqrt{H^2 + (d + w')^2} \tag{28}$$

### 4 Methods/experimental

Figure 3 depicts the considered measurement setup schematically. The setup is similar to that of [36–38], although we here consider arrays of bricks and bonsai trees.

We considered a frequency band from 38 to 40 GHz and assumed the following values:  $n = 1-3-5$ ,  $d = 1$  m ( $130\lambda$ ),  $w = 69.9$  cm ( $90.9\lambda$ ), and *hard*/vertical polarization.

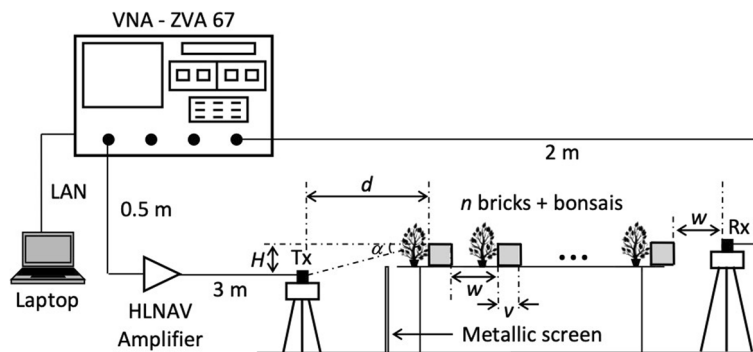


**Fig. 3** Measurement setup

The brick width was  $v = 5.1$  cm, and the canopies of the five bonsai trees were on average 20.8 cm ( $27\lambda$ ) wide and 14.6 cm ( $19\lambda$ ) high, with an average leaf width of 2.3 cm ( $3\lambda$ ). To create a negative incidence, we varied the transmitting antenna's height  $H$  from 0 m to  $-0.05$  m ( $5.2\lambda$ ) in 0.01 m ( $1.3\lambda$ ) increments (six positions), which provided attenuation relative to the free-space field strength for all considered  $H$  values. The resulting maximum incident angle  $\alpha$  value of  $-2.86^\circ$  is appropriate for analyzing multiple diffraction scenarios. We used 293 frequency points to assess the channel frequency response; these points were regularly spaced along the 38–40 GHz range. As a result, there was no time aliasing when the maximum distance of  $293/\text{BW} \cdot 3e8 = 44$  m was measured; notably, the measurement environment's maximum dimension was 7 m.

For the measurements, we used STEATITE Q-par 0.8–40 GHz omnidirectional antennas [39], which had a  $-2.2$ – $6.9$  dBi gain range. It should be noted that a far-field characterization was assumed. As the antennas' maximum dimension was  $D < 6$  cm, the far field began at  $2D^2/\lambda$  [1] [40], i.e., at a 0.93 m distance. As mentioned, we took 1 m as the distance existing between the transmitter and the first brick/bonsai pair. The power transmission of the Rohde and Swartz ZVA 10 MHz–67 GHz Vector Network Analyzer (VNA) [41] used here was  $-20$  dBm, and it had a 1000 Hz intermediate frequency. Due to our proper application of [36]'s time-gating technique, we were able to eliminate any undesirable contributions when selecting multiple diffraction contributions to compute the relative attenuation.

## 5 Results and discussion

Figure 4 presents the attenuation at the Rx in Fig. 3, relative to the space field, as a function of  $H$ . The figure presents a comparison of the attenuation obtained through the UTD–PO formulation for trees and rectangular sections, proposed in this study, and that derived from the measurements performed on the scaled bonsai/brick model.

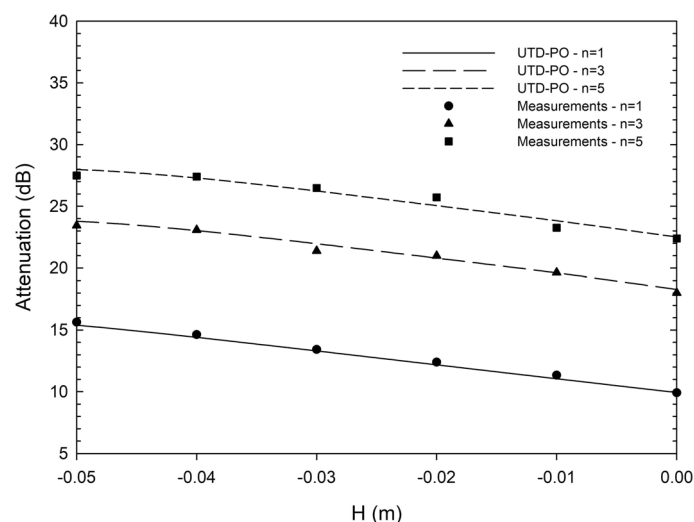


**Fig. 4** Attenuation based on the proposed UTD–PO solution for rectangular sections with trees, as a function of  $H$ , compared with the measurements performed on a scaled model. Considered parameters:  $f = 39$  GHz,  $n = 1$ – $3$ – $5$ ,  $w = 69.9$  cm,  $d = 1$  m,  $v = 5.1$  cm, bricks' relative permittivity  $\epsilon_r = 4.37 + 0.04j$ , hard/vertical polarization and  $\Delta d = 9$  cm; the COST 235 foliage attenuation model was considered for the in-leaf case



We considered the following parameters:  $f = 39$  GHz,  $n = 1-3-5$ ,  $w = 69.9$  cm,  $\nu = 5.1$  cm,  $d = 1$  m, bricks' relative permittivity  $\epsilon_r = 4.37 + 0.04j$  [42],  $\Delta d = 9$  cm, and hard/vertical polarization; the COST 235 foliage attenuation model was considered for the in-leaf case. As we assumed a 0.01 m step for the experimental data, and considering the used frequency (39 GHz), there is nearly one measurement per wavelength; this is adequate to produce accurate results. Our findings reveal a solid agreement between the model measurements and the theory-based formulations for all three considered  $n$  values. In this sense, it is also noteworthy that the agreement between the UTD-PO model predictions and the experimental measurements is remarkably consistent across different values of  $n$ . Moreover, as the number of obstacles increases, there's a noticeable rise in attenuation, particularly as  $H$  becomes more negative. This is indicative of the wave encountering more blockage from the rectangular sections and the tree canopies as the angle of incidence becomes increasingly negative, leading to higher energy being obstructed and, consequently, a reduced signal strength at the reference point.

## 6 Conclusion

We present a UTD-PO formulation that is based on Babinet's principle for the estimation of the multiple diffraction attenuation of radiowaves due to the presence of buildings and trees in an urban setting with vegetation, assuming spherical-wave incidence from a transmission source situated at a low height. The buildings and trees were modeled as rectangular sections which include the influence of vegetation through the corresponding attenuation factors and phasors, and the solution was validated through a comparison between the attenuation predictions and measurements on a scaled model of the considered environment performed at 39 GHz; the obstacles were hereby modeled using bricks and bonsai trees. The presented formulation is particularly useful in that, because of recursion, merely single diffractions are required for the estimation, thereby bypassing the need for higher-order diffraction terms within the expressions of the diffraction coefficients. This reduces the computing time and power needed for the estimations.

Our findings may be of great value for use in the planning of mobile communication systems in the future, even going beyond 6G networks. Thus, the enhanced understanding and precise modeling of radiowave propagation phenomena as influenced by urban structures and vegetation can lead to more reliable and efficient network designs. This, in turn, could lead to improved quality of service for end-users, as well as cost savings for network operators due to more accurate deployment strategies.

Looking ahead, there are several promising avenues for further research. One potential direction involves extending our UTD-PO formulation to incorporate different types of vegetation with varying densities and heights, which could provide a more comprehensive understanding of their impact on wave propagation. Another avenue could be the exploration of our model's applicability to other frequency bands, particularly those envisioned for use in future wireless communication technologies. Additionally, investigating the effects of varying urban layouts and building materials on radiowave propagation would further enhance the utility of our model. Finally, integrating our findings into larger-scale network simulation tools could offer insights into the design and optimization of next-generation wireless networks.

### Abbreviations

UTD	Uniform theory of diffraction
PO	Physics optics
6G	Sixth generation
MD	Multiple diffraction
UHF	Ultra-high frequency
LOS	Line of sight

### Acknowledgements

Not applicable.

### Author Contributions

JLL wrote the manuscript and performed calculations and formulation; JVR contributed to the formulation and assisted in manuscript writing; MTMI and JMGP helped with experimental measurements; IRR contributed to the simulation code; LJJ provided the theoretical foundation of UTD-PO. All authors read and approved the final manuscript. Authors Information Not applicable.

### Funding

This work was supported by the Ministerio de Ciencia e Innovación, Spain, under Grant PID2022-136869NB-C32 funded by MCIN/AEI/10.13039/501100011033 and by the European Union.

### Availability of data and materials

No external materials or data.

### Declarations

#### Competing interests

The authors declare that there are no competing interests.

Received: 6 January 2024 Accepted: 13 June 2024

Published online: 20 June 2024

### References

1. T.S. Rappaport, *Wireless Communications: Principles and Practice* (Prentice-Hall, Upper Saddle River, 2002)
2. A.F. Molisch, *Wireless Communications* (John Wiley & Sons, 2012)
3. Y. Xiao et al., Millimeter wave communications for future mobile networks. *IEEE J. Select. Areas Commun.* **35**(9), 1909–1935 (2017)
4. A. Goldsmith, *Wireless Communications* (Cambridge University Press, 2005)
5. J. Walfisch, H.L. Bertoni, A theoretical model of uhf propagation in urban environments. *IEEE Trans. Ant. Prop.* **36**(12), 1788–1796 (1988)
6. H.H. Xia, A simplified analytical model for predicting path loss in urban and suburban environments. *IEEE Trans. Veh. Technol.* **46**(4), 1040–1046 (1997)
7. S.R. Saunders, F.R. Bonar, Prediction of mobile radio wave propagation over buildings of irregular heights and spacings. *IEEE Trans. Antennas Propag.* **42**(2), 137–144 (1994)
8. M.J. Neve, G.B. Rowe, Contributions towards the development of a UTD-based model for cellular radio propagation prediction. *IEE Proc. Microw. Antennas Propag.* **141**(5), 407–414 (1994)
9. J.V. Rodriguez et al., A new solution expressed in terms of UTD coefficients for the multiple diffraction of spherical waves by a series of buildings. *Radio Sci.* **42**, RS4011 (2007)
10. C. Puente-Baliarda, J. Romeu, R. Pous, A. Cardama, On the behavior of the sierpinski multiband fractal antenna. *IEEE Trans. Antennas Propag.* **46**(4), 517–524 (1998)
11. J. Anguera, C. Borja, C. Puente, Microstrip fractal-shaped antennas: a review, in *The Second European Conference on Antennas and Propagation, EuCAP (2007)*. (IET, 2007), p. 1–7
12. E. Guariglia, Harmonic sierpinski gasket and applications. *Entropy* **20**(9), 714 (2018)
13. E. Guariglia, Entropy and fractal antennas. *Entropy* **18**(3), 84 (2016)
14. M.V. Berry, Z.V. Lewis, J.F. Nye, On the Weierstrass–Mandelbrot fractal function. *Proc. R. Soc. Lond. A Math. Phys. Sci.* **370**(1743), 459–484 (1980)
15. E. Guariglia, S. Silvestrov, Fractional-wavelet analysis of positive definite distributions and wavelets on  $\mathcal{D}'(\mathbb{C})$ , in *Engineering Mathematics II*, ed. by S. Silvestrov, M. Rancic (Springer), p. 337–353
16. S.R. Best, Operating band comparison of the perturbed Sierpinski and modified Parany gasket antennas. *IEEE Antennas Wirel. Propag. Lett.* **1**, 35–38 (2002)
17. W.J. Krzysztofik, Fractal geometry in electromagnetics applications—from antenna to metamaterials, *Microw. Rev* **192** (2013)
18. E. Guariglia, Primality, fractality and image analysis. *Entropy* **21**(3), 304 (2019)
19. R.G. Hohlfeld, N. Cohen, Self-similarity and the geometric requirements for frequency independence in antennae. *Fractals* **7**(01), 79–84 (1999)
20. N. Savage et al., Radio wave propagation through vegetation: factors influencing signal attenuation. *Radio Sci.* **38**(5), 9–1 (2003)

21. Y. Xu et al., Analysis of propagation and diffraction rule of radiofrequency signal in man-made forest. *Trans. Chin. Soc. Agric. Eng.* **31**(4), 224–231 (2015)
22. M. Ghorraishi et al., *Radio Wave Propagation Through Vegetation* (IntechOpen, 2013)
23. R.F. Caldeirinha, *Radio Characterisation of Single Trees at Micro-and Millimetre Wave Frequencies*, Ph.D. dissertation, University of South Wales (United Kingdom), (2001)
24. E.S. Malevich et al., A new discrete model of the forest environment for predicting the radio-wave propagation and its statistical characteristics, in *2020 International Youth Conference on Radio Electronics, Electrical and Power Engineering (REEPE)* (IEEE, 2020), p. 1–6
25. W. Zhang, Formulation of multiple diffraction by trees and buildings for radio propagation predictions for local multipoint distribution service. *J. Res. Natl. Inst. Stand. Technol.* **104**(6), 579–585 (1999)
26. S.A. Torrico et al., Modeling tree effects on path loss in a residential environment. *IEEE Trans. Ant. Prop.* **46**(6), 872–880 (1998)
27. A. Ghorbani et al., A new uniform theory of diffraction based model for multiple building diffraction in the presence of trees. *Electromagnetics* **31**, 127–146 (2011)
28. K.L. Chee et al., Radiowave propagation prediction in vegetated residential environments. *IEEE Trans. Veh. Technol.* **62**(2), 486–499 (2013)
29. I. Rodriguez-Rodriguez et al., Validation with measurements of plane and spherical-wave UTD–PO propagation models which assume flat-topped obstacles. *AEU-Int. J. Electron. Commun.* **85**, 174–178 (2018)
30. D. Erricolo et al., Measurements on scaled models of urban environments and comparisons with ray-tracing propagation simulation. *IEEE Trans. Antennas Propag.* **50**(5), 727–735 (2002)
31. M.T. Martinez-Ingles et al., UTD–PO solution for estimating the propagation loss due to the diffraction at the top of a rectangular obstacle when illuminated from a low source". *IEEE Trans. Antennas Propag.* **61**(12), 6247–6250 (2013)
32. J.V. Rodriguez et al., UTD–PO solutions for the analysis of multiple diffraction by trees and buildings when assuming spherical-wave incidence. *Electronics* **12**, 4 (2023)
33. R.G. Kouyoumjian, P.H. Pathak, A uniform geometrical theory of diffraction for an edge in a perfectly conducting surface. *Proc. IEEE* **62**(11), 1448–1461 (1974)
34. Radio propagation effects on next-generation fixed-service terrestrial telecommunication systems. Final Report, Luxembourg, (1996)
35. C. Matzler, Microwave (1–100 GHz) dielectric model of leaves. *IEEE Trans. Geosci. Rem. Sens.* **32**(5), 947–949 (1994)
36. M.T. Martinez-Ingles et al., Comparison of a UTD–PO formulation for multiple-plateau diffraction with measurements at 62 GHz. *IEEE Trans. Antennas Propag.* **61**(2), 1000–1003 (2013)
37. M.T. Martinez-Ingles et al., Experimental and theoretical comparison of cylindrical against rectangular obstacles in mm-wave multiple diffraction. *IEEE Trans. Antennas Propag.* **61**(10), 5347–5350 (2013)
38. M. Martinez-Ingles et al., On the influence of diffuse scattering on multiple-plateau diffraction analysis at mm-wave frequencies. *IEEE Trans. Antennas Propag.* **67**(4), 2130–2135 (2019)
39. Steatite Antennas, QOM-SL-0.8-40-K-SG-L Datasheet, 2017, <https://www.steatite-antennas.co.uk/wp-content/uploads/2017/09/QOM-SL-0.8-40-K-SG-L.pdf>
40. C.A. Balanis, *Antenna Theory: Analysis and Design* (Wiley, New York, 1997)
41. Rohde & Schwarz, ZVA Product Homepage, 2023, [https://www.rohde-schwarz.com/es/producto/zva-pagina-de-inicio-producto\\_63493-9660.html](https://www.rohde-schwarz.com/es/producto/zva-pagina-de-inicio-producto_63493-9660.html)
42. A.V. Alejos et al., Measurement and analysis of propagation mechanisms at 40 GHz: viability of site shielding forced by obstacles. *IEEE Trans. Veh. Technol.* **57**(6), 3369–3380 (2008)

## Publisher's Note

Springer Nature remains neutral with regard to jurisdictional claims in published maps and institutional affiliations.